Title
MORPHOLOGY, CRYSTALLOGRAPHY AND FORMATION OF DISLOCATED (LATH) MARTENSITES IN STEELS

Author
Thomas, G.

Publication Date
1977-05-01

LBL-6242
Preprint

Presented at the International Conference
on Martensitic Transformations, Kiev,
USSR, May 16-20, 1977

MORPHOLOGY, CRYSTALLOGRAPHY AND FORMATION OF DISLOCATED (LATH) MARTENSITES IN STEELS

G. Thomas and B. V. N. Rao

May 1977

Prepared for the U. S. Energy Research and
Development Administration under Contract W-7405-ENG-48

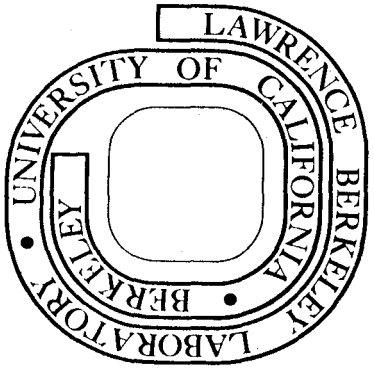

DISCLAIMER

MORPHOLOGY, CRYSTALLOGRAPHY AND FORMATION OF DISLOCATED (LATH) MARTENSITES IN STEELS*

G. Thomas and B.V.N. Rao

Department of Materials Science and Mineral Engineering, College of Engineering, and Materials and Molecular Research Division, Lawrence Berkeley Laboratory, University of California, Berkeley, Ca. 94720.

I. INTRODUCTION

Although the morphology and crystallography of plate martensites are well understood, the same is not true for the dislocated lath martensites occurring in the technologically more important medium and low carbon steels (1,2,3). This paper is concerned with a detailed electron diffraction and microscopy examination of dislocated lath martensites and has been partly stimulated by the detection of small amounts of retained austenite (4) in many lath martensites during an extensive alloy design program on dislocated martensitic steels (2). Consequently, the unique orientation relationships can be obtained directly by utilizing selected area diffraction (SAD) analyses of the lath bundles and the surrounding austenite. Such analysis is more precise at high voltages due to the reduction of spherical aberration. This method serves to eliminate controversies that must arise if indirect methods of habit plane analysis are used (3,5-12). There is a wide scatter in the existing data as can be seen from Table I.

II. EXPERIMENTAL

The steels used in the present studies are given in Table II. Iron-nickel alloys in the form of 5 mil thick sheets encapsulated in evacuated quartz tubes, were austenitized 1 hr. at 1100°C and quenched into iced water. The carbon steels were austenitized in bulk for 1 hr. followed by quenching into iced water. Different austenitizing temperatures were used to change grain sizes. Details about the heat-treatment and specimen preparation are described elsewhere (e.g. 13).

III. RESULTS

A. Morphology and Cell Structure of Martensite - The martensite packet size was found by optical microscopy to increase with austenitizing temperature and prior austenite grain size (Table III) but did not show the same rate of increase as the prior austenite grain size when the austenitizing temperature was increased from 870 to 1200°C. There was no noticeable variation in the average lath width as a function of prior austenite grain size.

Transmission electron micrographs taken at 100kV and 500kV revealed that the laths are parallel with reasonably straight boundaries and a high dislocation density (Figs. 1 and 2). Although there were no significant differences in lath morphology or substructure as a function of carbon content, retained austenite could only be detected in the carbon containing alloys (cf. Figs. 1 and 2), in agreement with Yeo (14). Fig. 2 gives evidence of retained austenite in the ternary Fe-4Cr-0.3C alloy (Fig. 2a through c) and quaternary Fe-4Cr-2Mn-0.3C alloy (Fig. 2d through f). Indexed diffraction patterns clearly reveal the austenite zones (110) (Fig. 2c) and (211) (Fig. 2f). A detailed discussion of the identification of small quantities of retained austenite has been published elsewhere (4,15), where it is emphasized that great care is needed to detect and uniquely identify these austenite films.

* Invited paper, International Conference on Martensite, Kiev, USSR, May 1977. Work supported by ERDA through MMRD, LBL.

B. Crystallography of the Transformation

1) Relative Orientations of Adjacent Laths: Fig. 1 is an example of a detailed analysis of parallel laths. The SAD patterns and regions from where the patterns are obtained in the bright-field image are identified by 1,2,3 etc. The $[110]\alpha^*$ crystal direction remains parallel in all the laths in this packet, indicating that these laths are separated by $[110]\alpha$ rotation boundaries. Using stereographic analysis, it is found that lath 5 is rotated 180° with respect to lath 1 indicating that the shear components are opposite and accommodative. Thus within the packet the relative orientations of laths is such as to minimize the overall shape deformation. However the rotation axis for producing adjacent lath orientations is not uniquely $[110]\alpha$, since $[100]\alpha$ is also observed. It is possible that adjacent laths can be twin related (12) in which case a 180° rotation of shear vector is obtained in a single step at adjacent laths but twin related adjacent laths are found to occur infrequently in the present investigation.

2) Austenite/Martensite Orientation Relationships: The ternary Fe-4Cr-0.3C alloys showed the K-S (Kurdjumov-Sachs) relation (Fig. 2c) while alloys modified with 2% Mn and 5% Ni (alloys 5 and 6) revealed the N-W (Nishiyama-Wasserman) relation (Fig. 2f). In Fig. 2c there are two martensite zones, $[100]\alpha$ and $[111]\alpha$, and yet a single $[110]\gamma$ zone. The $[111]\alpha$ and $[110]\gamma$ combination results in K-S relation, but if $[100]\alpha$ and $[110]\gamma$ are considered, the result is the N-W relation. It is clear, therefore, that this is an ambiguous pattern for orientation relationship analysis although this is not apparently well recognized by other workers. K-S relation in the ternary alloy is, however, concluded from several unambiguous diffraction patterns (4, 15).

3) Trace Analysis: Fig. 3c shows the trace analysis directly in austenite from which it can be seen that the habit plane in austenite is very close to the $(111)\gamma$ within the limits of the accuracy of the electron metallographic trace analysis (2°). This habit plane in the parent phase agrees with several earlier investigators (Table I). A determination of the habit direction of the laths in austenite indicates that it falls closely along $[\bar{1}10]\gamma$ .Figure 3a shows the scatter when trace analysis is done only in martensite and emphasises the advantages of detecting and utilizing the retained austenite. Figure 3b shows the trace analysis of the long axes of laths; these are always in $\langle 111\rangle\alpha$ within experimental error.

IV. DISCUSSION

Because packet size increases at constant lath width (Table III), the aspect ratio of the laths increases with prior austenite grain size. A constant aspect ratio with increasing packet size would result in a higher volume dependent strain energy.

The present observations suggest that the orientations of the laths in a given packet are those which result from minimization of the overall shape deformation and its accommodation over a group of laths. Analysis of several adjacent laths in a packet was necessary to reach this conclusion. It is also shown that a gradual change in orientation to minimize shape deformation is preferred to a twin orientation of the adjacent laths.

The habit plane by direct trace analysis is shown to be $\{111\}\gamma$. Some of the scatter in the habit plane analysis by indirect methods may be due to the presence of ledges in the austenite-martensite interface as shown in Fig. 4a. From this figure, the microscopic habit plane

* The subscripts α and M refer to martensite and γ and A refer to austenite.

remains {111}γ but the macroscopic habit plane of any {hkl}γ can be generated by varying ledge density, ledge morphology, or both as shown in Figs. 4b and c. The martensite laths would thicken by propagation of these ledges into the surrounding austenite.

The identification of retained austenite around the lath boundaries supports the view that these laths are indeed individual nucleation events. The proponents of the idea that a packet is a fundamental growth unit (16,17) derive their support largely from the observation that surface relief experiments reveal upheavals over distances which are often 5 to 6 lath widths. However, as shown by the present study, adjacent laths may be rotated with respect to a common axis. Therefore although all the individual laths undergo shear, they contribute to surface relief only over distances which are 5 to 6 laths in width. From these arguments, it appears that the so-called laths are really small platelets as shown in Fig. 5. In the case of carbon steels the laths are separated by thin films of austenite which are stabilized largely due to the segregation of carbon from the adjoining laths as indicated in the diagram.

V. CONCLUSIONS

1. The aspect ratio of the lath martensite increases with prior austenite grain size. This is a lower strain energy configuration than if the aspect ratio were to be maintained constant.

2. The orientation of adjacent laths in a packet is the result of minimization of the overall shape deformation. This is not normally achieved by a single step twin mechanism but most commonly through a multi-step orientation process involving rotation of adjacent laths along a common axis such that the shear vector completes a 2π rotation in a group of adjacent laths (several cycles possible within a packet).

3. Both {110}α and {331}α habit planes are observed.

4. Retained austenite is found in all the carbon containing alloys. It is found to exhibit either Kurdjumov-Sachs or Nishiyama-Wasserman orientation relationship with the martensite, depending on composition.

5. Direct habit plane analysis in austenite yielded a single interface plane; {111}γ. It is suggested that the austenite-martensite interface may be a ledge boundary and that the "macroscopic" and "microscopic" habit planes could be different.

6. It is concluded that martensite laths are thin platelets and that individual laths and not the packets are the fundamental nucleation events.

ACKNOWLEDGEMENTS

We are grateful to M. Carlson for his help and for use of some of his unpublished work. Helpful discussions with Dr. David Clarke, Dr. R. Gronsky and Professor A. Khachaturyan are appreciated.

REFERENCES

1. C. W. Wayman: Metallography, 1975, vol. 8, p. 105.
2. G. Thomas: Iron and Steel Intl., 1973, vol. 46, p. 451.
3. A. B. Grenninger and A. R. Troiano: Trans. AIME, 1940, vol. 140, p. 307.
4. B.V.N. Rao, J. A. Koo and G. Thomas: Proc. Electron Microscopy Society of America, 33rd Annual Meeting, p. 30, Claitors Publishing Division, Baton Rouge, 1975.
5. D. S. Sarma, J. A. Whiteman, and J. H. Woodhead: Metal Sci. J., 1976, vol. 10, p. 391.
6. R. F. Mehl, C. Barrett, and D. W. Smith, Trans AIME, 1933, vol. 105, p. 215.
7. F. J. Schoen, J. L. Nilles and W. S. Owen, Met. Trans., 1971, vol. 2, p. 2489.
8. A. R. Marder and G. Krauss: Trans. ASM, 1969, vol. 62, p. 957
9. P. M. Kelly and J. Nutting, Proc. Roy. Soc., 1960, vol. A259, p. 45.
10. T. Bell and W. S. Owen: JISI, 1967, vol. 205, p. 428.
11. J. D. Bolton and E. R. Petty: Metal Sci. J., 1971, vol. 5, p. 166.
12. J. M. Chilton, C. J. Barton and G. R. Speich: JISI, 1970, vol 208, p 184.
13. B.V.N. Rao, R. W. Miller and G. Thomas: Proc. of 16th Intl. Heat Treatment Conf., "Heat Treatment '76", The Metals Scoeity (London), p 75.
14. R. B. G. Yeo: Trans. AIME, 1962, vol. 224, p. 1222.
15. G. Thomas: To be published in Met. Trans., Univ. of California, Berkeley, LBL Report #5732.
16. M. J. Roberts: Met. Trans., 1970, vol. 1, p. 3287.
17. J. S. Pascover and S. V. Radcliffe: Acta Met., 1969, vol. 17, p. 321.

TABLE I. SUMMARY OF CRYSTALLOGRAPHIC STUDIES IN LATH MARTENSITE

Investigator(s)	Habit Plane in Martensite	Habit Plane in Austenite	Ref.
Mehl et al.	____	{111}γ	6
Greninger & Troiano	____	{111}γ	3
Schoen et al.	____	{111}γ	7
Marder & Krauss	____	{557}γ	8
Kelly & Nutting	<111>α*	<110>γ*	9
Bell & Owen	{110}α	____	10
Bolton & Petty	{110}α	____	11
Chilton et al.	{213}α	____	12
Sarma et al.	{213}α	____	5

* long direction of the needle/lath

TABLE II. CHEMISTRY OF THE ALLOYS AND THEIR Ms TEMPERATURES

Alloy #	Alloy Comp. (wt%), Nominal	Ms (°C)
1)	Fe-12 Ni	300 *
2)	Fe-15 Ni	250 *
3)	Fe-20 Ni	165 *
4)	Fe-4Cr-0.3C	320
5)	Fe-4Cr-5Ni-0.3C	210
6)	Fe-4Cr-2Mn-0.3C	253

* calculated

TABLE III. VARIATION OF MARTENSITE SIZE PARAMETERS WITH AUSTENITIZING TREATMENT IN Fe/4Cr/0.3C Alloy

Austenitizing temperature (°C)	Prior austenite grain size, μm	Martensite packet size, μm	Martensite lath width μm
870	29	26	0.37
1000	111	31	0.35
1100	202	42	0.39
1200	254	47	0.39

FIGURE CAPTIONS

Fig. 1 (a) Parallel laths in a packet martensite (Alloy 1). The [110]M remains the same in all the laths of the region. BF micrograph. (b) Corresponding indexed SAD patterns with the electron zone axes shown in the top left circles.

Fig. 2 (a), (b) and (c): BF, DF and SAD pattern revealing retianed austenite in alloy 4. DF (b) is obtained using (002)γ reflection in (c). (d), (e), (f): BF,DF and SAD pattern showing retained austenite in alloy 6. DF(e) is obtained using $(02\bar{2})$ reflection of the [211]γ zone. N-W orientation relationship is shown in (f).

Fig. 3 Trace analysis of habit plane/direction for the martensite transformation, (a) analysis of plane in martensite showing (011)α and (133)α habits, (b) analysis of direction in martensite showing near [111]α habit, (c) direct analysis of plane in aprent austenite revealing near (111)γ habit.

Fig. 4 (a) Suggested ledge model of the austenite/martensite interface (b) and (c) show different ledge configurations leading to either different macroscopic and microscopic habit planes (b) or a single habit plane(d).

Fig. 5 Proposed morphology of lath martensite, b>a>>c. Arrows indicate C segregation into austenite (A) from adjoining martensite (M).

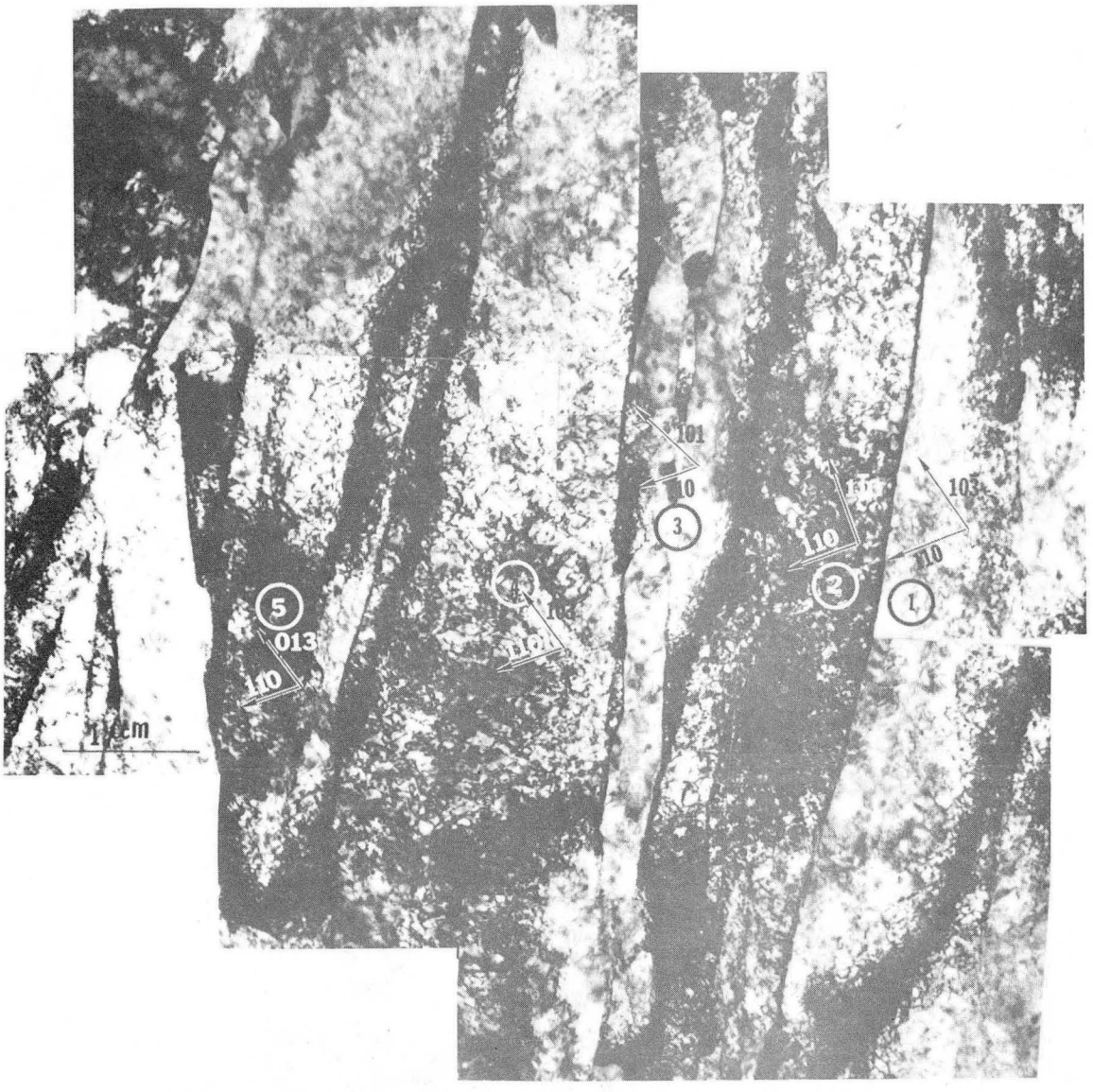

XBB 775 4292

Fig. 1(a)

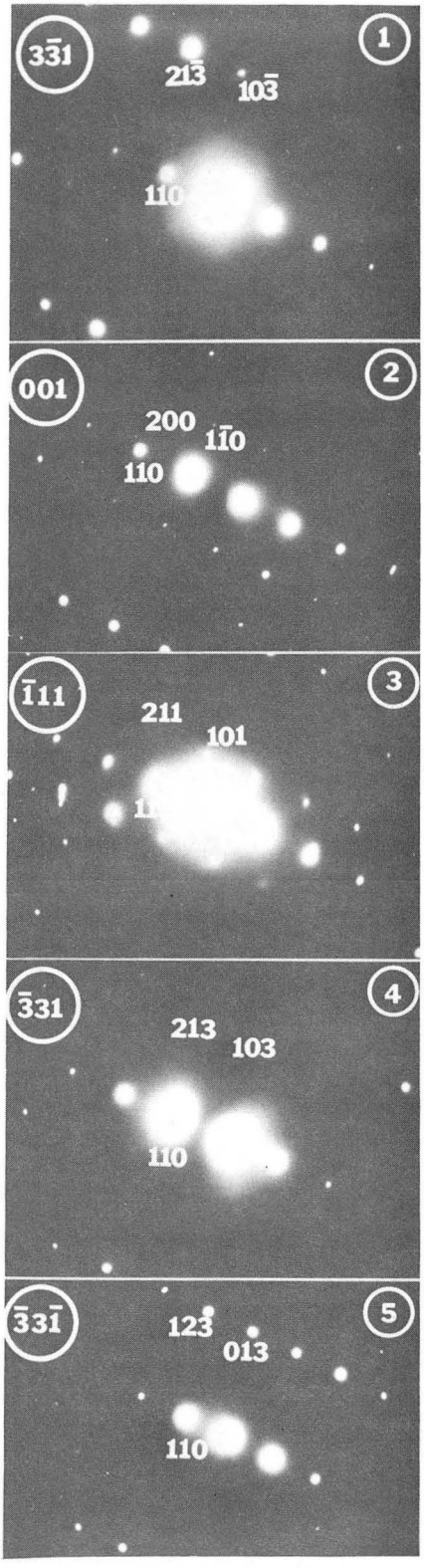

XBB 775-4293

Fig. 1(b)

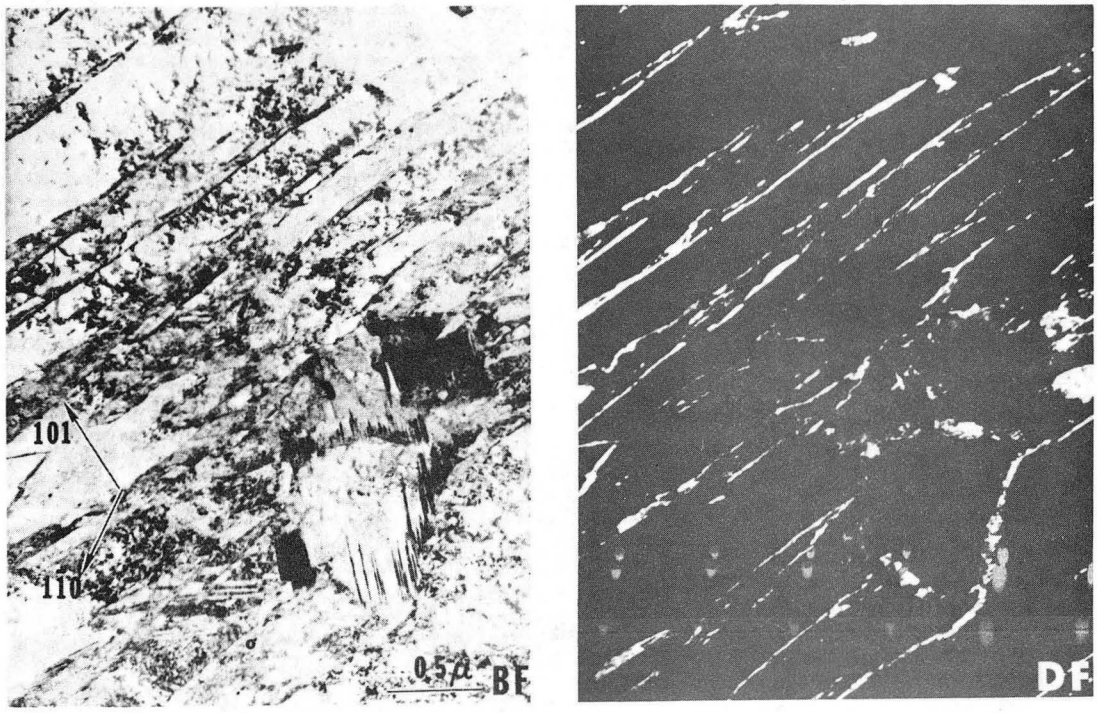

XBB 765-4568

Fig. 2(s) and (b)

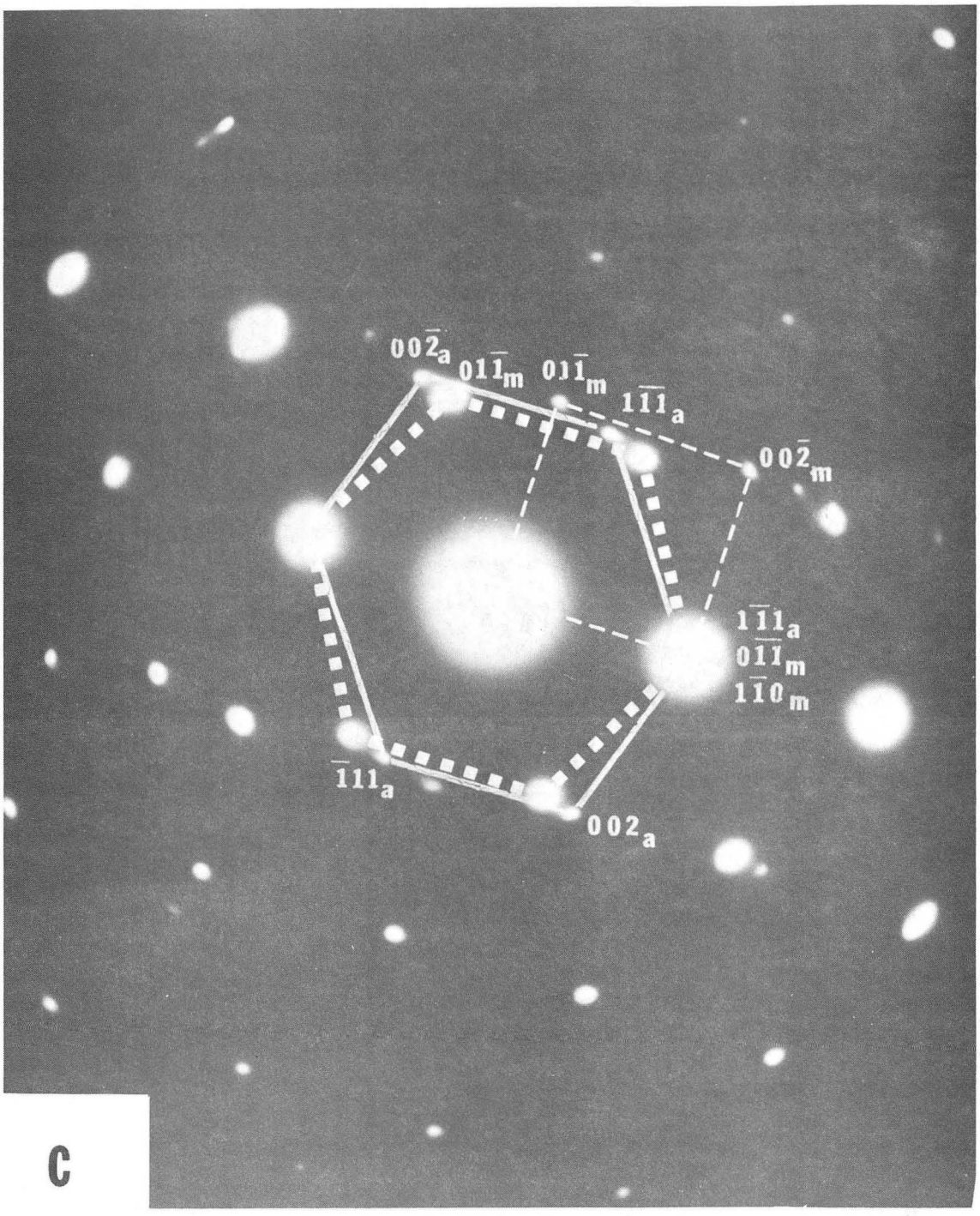

XBB 744-3113

Fig. 2(c)

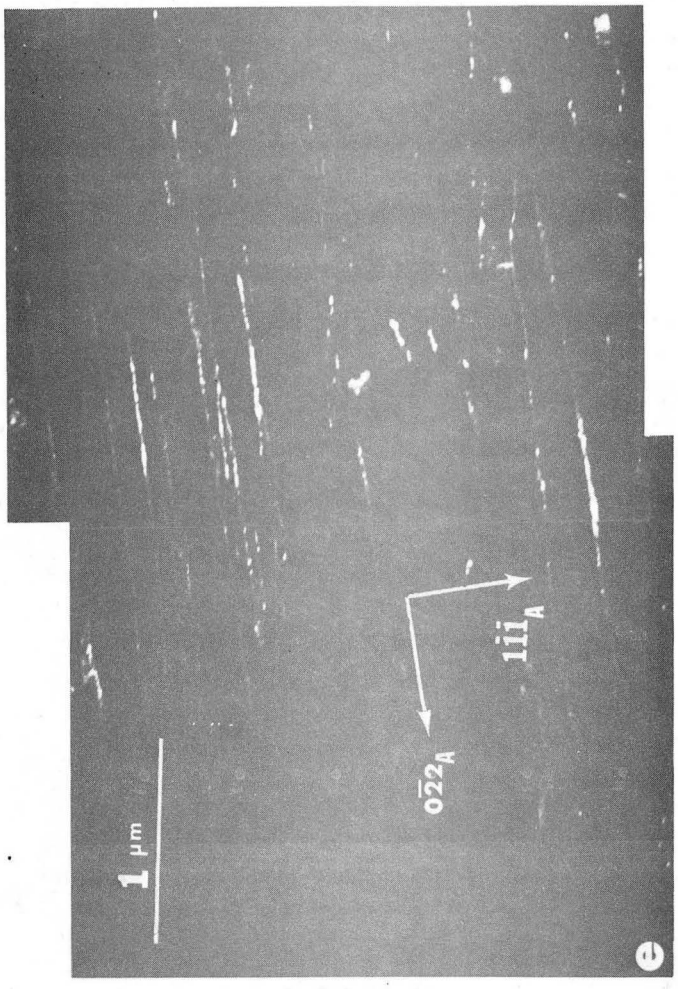

XBB 775-4291

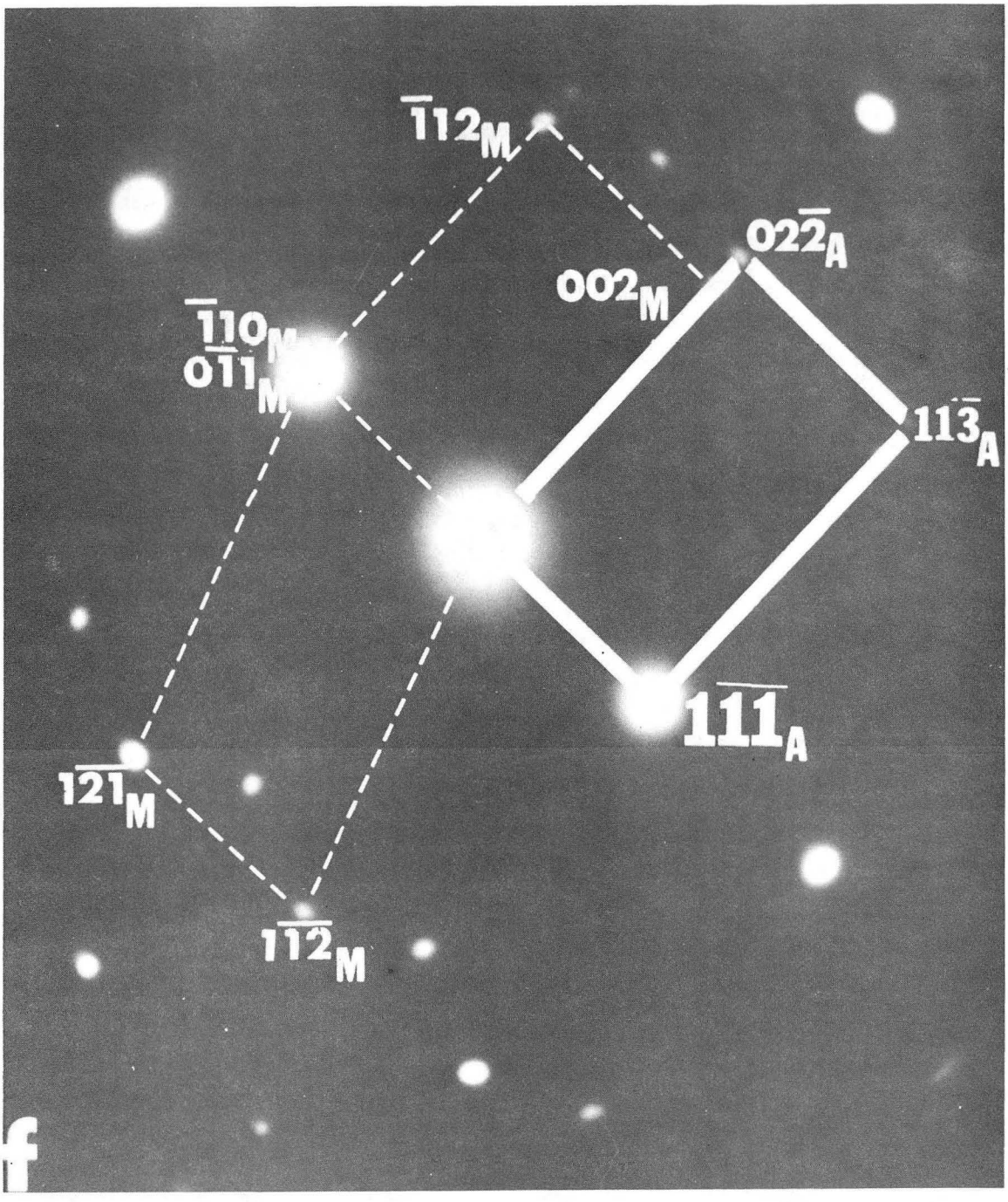

XBB 775-4290

Fig. 2(f)

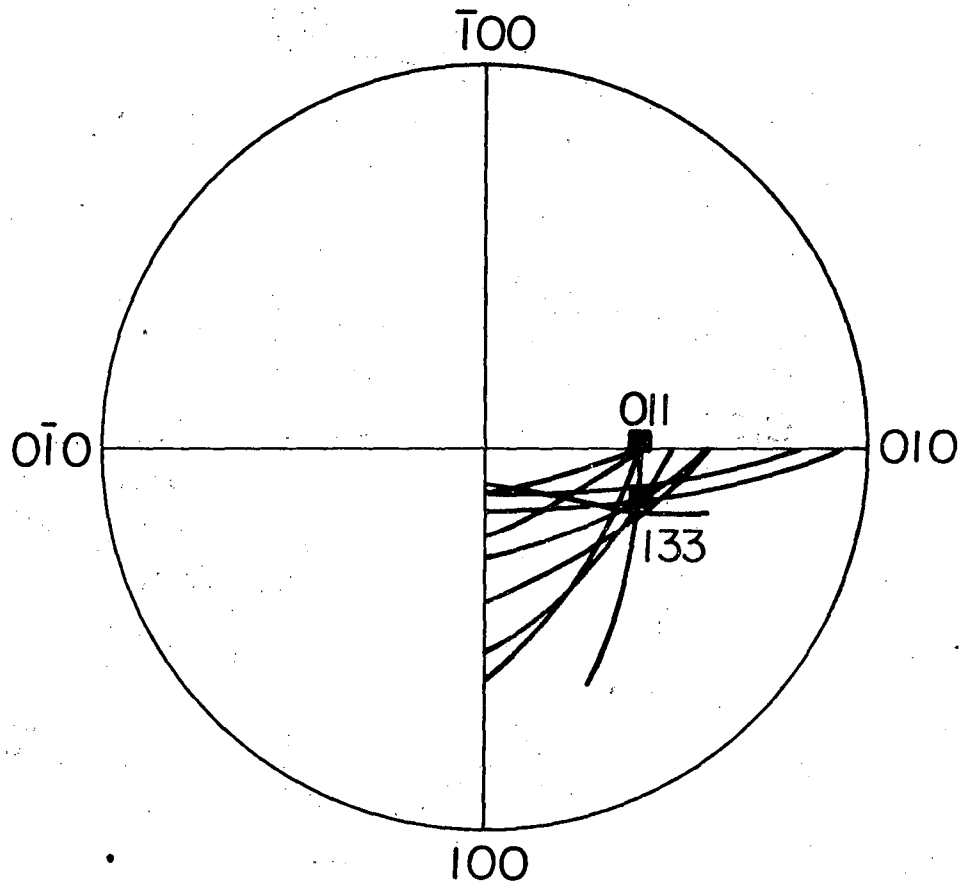

XBL774-5395

Fig. 3(a)

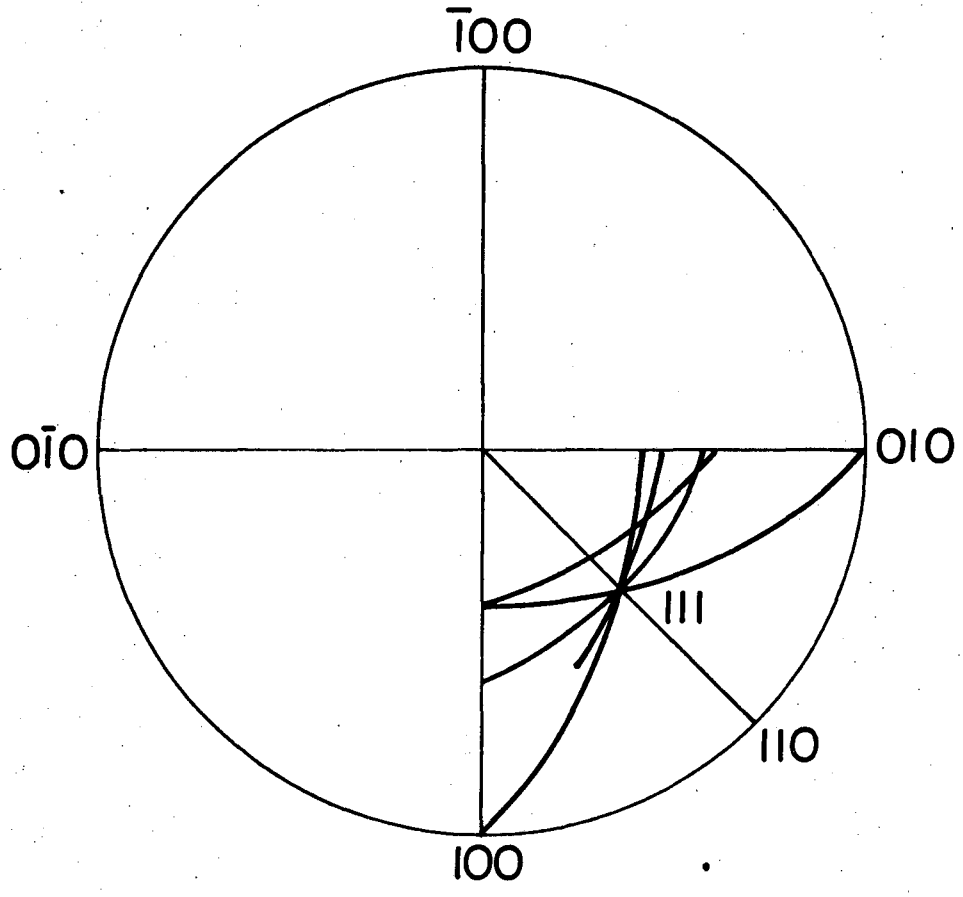

XBL 774-5396

Fig. 3(b)

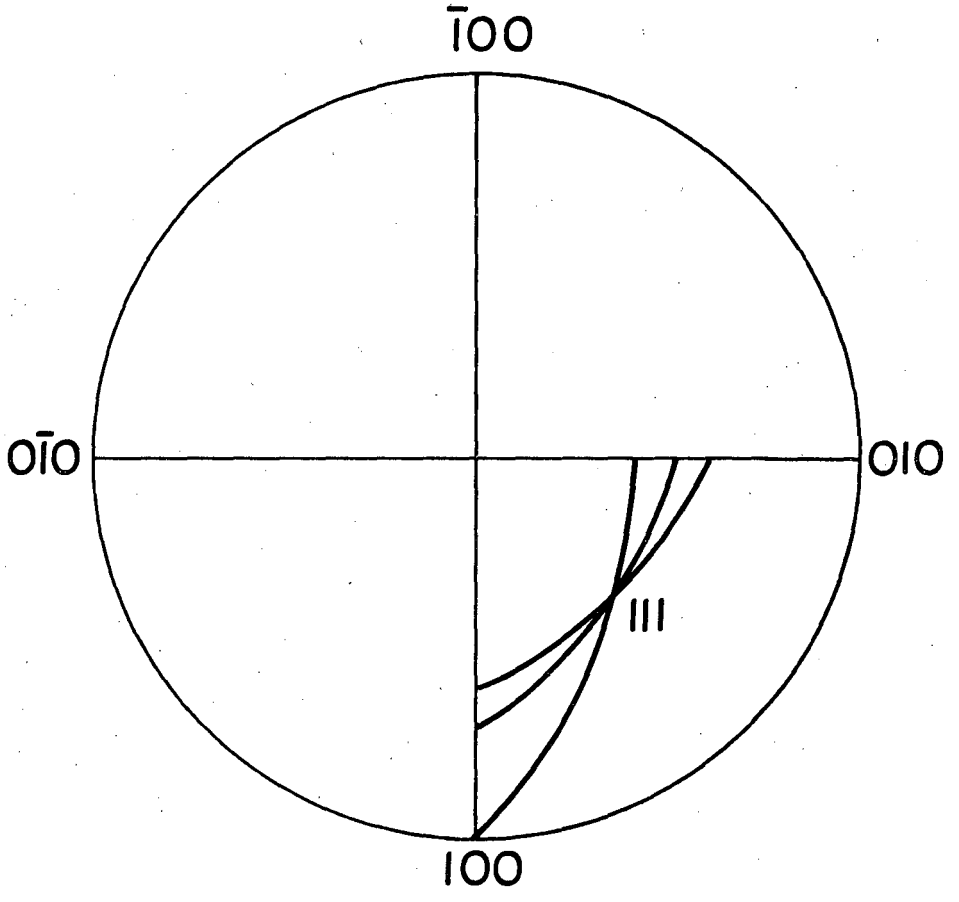

XBL 774-5397

Fig. 3(c)

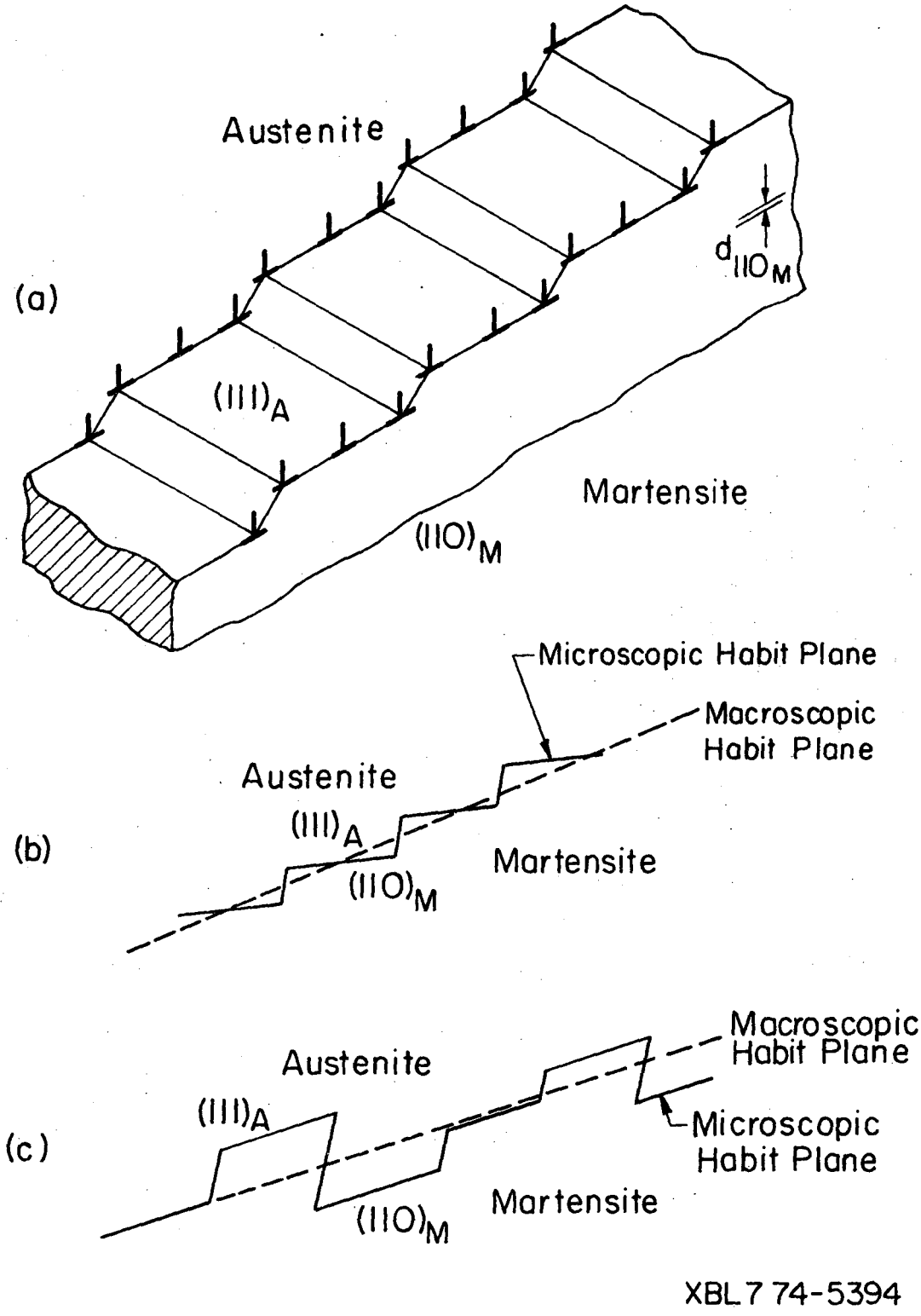
(a)
Austenite
d_{110_M}
$(111)_A$
Martensite
$(110)_M$
(b)
Microscopic Habit Plane
Macroscopic Habit Plane
Austenite
$(111)_A$
Martensite
$(110)_M$
(c)
Austenite
$(111)_A$
Macroscopic Habit Plane
Microscopic Habit Plane
Martensite
$(110)_M$
XBL7 74-5394

Fig. 4

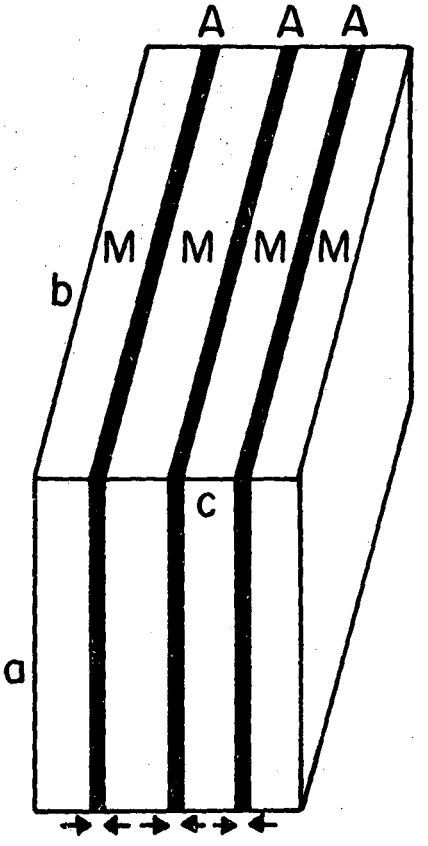

XBL 774-5393

Fig. 5

This report was done with support from the United States Energy Research and Development Administration. Any conclusions or opinions expressed in this report represent solely those of the author(s) and not necessarily those of The Regents of the University of California, the Lawrence Berkeley Laboratory or the United States Energy Research and Development Administration.

TECHNICAL INFORMATION DIVISION
LAWRENCE BERKELEY LABORATORY
UNIVERSITY OF CALIFORNIA
BERKELEY, CALIFORNIA 94720